Eur. Phys. J. B **6**, 317–322 (1998)

THE EUROPEAN PHYSICAL JOURNAL B

Magnetic susceptibility, heat capacity, and optical conductivity of LiPc and LiPcI

M. Dumm[1,a], M. Dressel[1,b], M. Nicklas[1], P. Lunkenheimer[1], A. Loidl[1], M. Weiden[2], F. Steglich[2], B. Assmann[3], H. Homborg[3], and P. Fulde[4]

[1] Institut für Physik, Elektronische Korrelationen und Magnetismus, Experimentalphysik V, Universität Augsburg, 86135 Augsburg, Germany
[2] Institut für Festkörperphysik, Technische Universität Darmstadt, 64289 Darmstadt, Germany
[3] Institut für anorganische Chemie, Christian-Albrechts Universität 24098 Kiel, Germany
[4] Max-Planck-Institut für Physik komplexer Systeme, 01187 Dresden, Germany

Received: 16 June 1998 / Accepted: 14 July 1998

Abstract. The magnetic susceptibility, using dc and electron spin resonance (ESR) methods, the specific heat, and the infrared properties of the one-dimensional molecular semiconductors lithium phthalocyanine (LiPc) and the iodinated compound LiPcI have been investigated for temperatures 1.5 K $\leq T \leq$ 300 K. LiPc has a half-filled conduction band and is expected to be an organic metal. However, due to the strong Coulomb repulsion the system is a one-dimensional Mott-Hubbard insulator with a Hubbard gap of 0.75 eV as inferred from optical measurements. The localized electrons along the molecular stacks behave like a $S = 1/2$ antiferromagnetic spin chain. The spin susceptibility, as determined by ESR experiments, and the magnetic contribution to the heat capacity show a Bonner-Fisher type of behavior with an exchange constant $J \approx 40$ K. LiPcI is an intrinsic narrow-gap semiconductor with an optical gap of 0.43 eV. In ESR experiments it is silent, indicating that all the unpaired electrons have been removed from the macrocycle via doping with iodine.

PACS. 76.30.-v Electron paramagnetic resonance and relaxation – 72.80.Le Polymers; organic compounds (including organic semiconductors) – 75.40.-s Critical-point effects, specific heats, short-range order

1 Introduction

Phthalocyanine (Pc) compounds have attracted much attention due to their large potentials for technical applications combined with low costs of production and a robust chemical and thermal stability. Metallophthalocyanines exist in insulating, semiconducting and even metallic phases and can be used, *e.g.*, as electrochromic devices, gas sensors, magnetic materials, or as constituents of molecular electronic devices (for a review see, *e.g.*, Refs. [1–3]). Phthalocyanines consist of macrocyclic molecules containing four pyrrole units which are connected *via* −N= bridges and are linked to one benzene ring each. In the inner macrocycle there are two NH groups, the hydrogen atoms of which can be substituted by a metal atom.

The synthesis of monoclinic LiPc was first reported by Homborg and Katz [4]. In LiPc the lithium ion is located at the center of the nearly planar molecule with both hydrogen atoms removed yielding an unpaired electron. It has been found that this extra electron is delocalized on the inner ring of the macrocycle [5]. The LiPc molecules are stacked metal to metal with an interplanar distance of 3.245 Å [6] which is significantly shorter than the van der Waals distance between the organic molecules [7]. Hence, one-dimensional electronic conduction should be expected along the stacking direction of the molecules due to a considerable overlap of the π orbitals of the Pc in this direction. Band-structure calculations predict a half-filled conduction band [8]. However, early dc conductivity measurements clearly revealed a semiconducting behavior with an energy gap of approximately 0.2 eV; the room-temperature conductivity σ is of the order of 10^{-2} to 10^{-3} $(\Omega\text{cm})^{-1}$ [9,10]. In addition the room-temperature spectra of the polarized reflectivity provided experimental evidence for an optical gap of approximately 0.5 eV. From the optical excitation spectrum the authors concluded that LiPc is a Mott-Hubbard insulator and calculated the on-site Coulomb energy $U = 1.5$ eV and the transfer energy $t = 0.3$ eV [11]. Detailed ac and dc conductivity measurements [12,13] gave evidence that one-dimensional variable-range hopping is the dominant dc transport mechanism. The magnetic properties were

[a] e-mail: `michael.dumm@physik.uni-augsburg.de`
[b] *Present address*: Physikalisches Institut, Universität Stuttgart, 70550 Stuttgart, Germany.

determined by dc SQUID measurements [7,14] and by ESR experiments [14,15]. From SQUID measurements a Curie-Weiss type of behavior of the susceptibility was deduced and has been described using concepts of spin fluctuations in band magnets [7]. Using ESR measurements, the influence of oxygen pressure on the ESR linewidth and the kinetics of oxygen absorption in LiPc has been elucidated.

Much less is known about the iodinated compound LiPcI. It has first been synthesized and characterized by Homborg and Teske [16]. LiPcI crystallizes in a tetragonal space group, with linear chains of equidistant iodine atoms which are segregated from adjacent stacks of the LiPc molecules. As all the unpaired electrons are removed from the Pc rings, intrinsic semiconducting behavior is expected. Again, based on ac transport measurements one-dimensional hopping conductivity was reported with a room-temperature dc conductivity $\sigma_{dc} = 0.2\ (\Omega\text{cm})^{-1}$ [12].

In this communication we study the optical conductivity, the magnetic susceptibility and the heat capacity in LiPc and LiPcI. For the first time we show that from the magnetic and thermodynamic properties, LiPc can be viewed as an almost ideal spin 1/2 antiferromagnetic Heisenberg chain. LiPcI is an intrinsic semiconductor characterized by a diamagnetic susceptibility.

2 Experimental details

For the synthesis of LiPc double distilled 1,2 dicyanobenzene (PDN) and lithium were heated to 150 °C. After the exothermic reaction was finished the reaction products were extracted with toluene, and LiPc needles remained in the residue. LiPcI was synthesized by heating double distilled PDN and LiI at 1450 °C for 15 h. The solid was extracted with dichloromethane. The lustrous needles of LiPcI were washed in ether and dried *in vacuo*. This polycrystalline needle-shaped material was investigated by ESR technique. For the dc susceptibility, transport, and optical experiments the LiPc and LiPcI powders were pressed into pellets.

The electron spin resonance measurements were performed using a conventional ESR spectrometer (Varian E-101) at X-band frequencies for temperatures 1.5 K $\leq T \leq$ 300 K and magnetic field sweeps from $0 \leq H \leq 10$ kOe. For cooling the sample down to 4.2 K, we used a He–flow cryostat. Below 4.2 K the experiments were carried out in a ^{4}He bath cryostat. The powdered samples were glued to a quartz rod with paraffin in order to achieve good thermal contact. Lithiumphthalocyanine is highly sensitive to absorbed oxygen which, however, is easily removed *in vacuo* [7,14,15]. To avoid effects of absorbed oxygen, the powdered samples were exposed to high vacuum over a period of several days; the sample handling was done in a glove box under argon atmosphere. The dc susceptibility was measured utilizing a commercial SQUID-magnetometer operating between 2 K and 300 K.

The low and high frequency transport measurements in the range 20 Hz $\leq \nu \leq$ 1 GHz were performed with four and two probe geometry as described in detail in reference [12]. In the infrared (IR) regime, the temperature dependent conductivity was determined *via* reflectivity measurements using a Bruker IFS 113v Fourier transform interferometer. The spectral range from 1 meV to 1 eV was covered utilizing a suitable set of three sources, six beamsplitters, two windows, and three detectors. The sample was placed in the exchange gas of a He bath cryostat going down to $T = 2$ K; a gold mirror served as reference. In order to take the surface roughness of the pressed pellet into account, the sample was subsequently covered with gold and the experiments were repeated. From the reflectivity data, the conductivity as well as the dielectric constant were calculated by the Kramers-Kronig analysis assuming a constant reflectivity at low frequencies and a ν^{-2} extrapolation at the higher end.

The heat-capacity measurements on LiPc were performed in a home-built adiabatic Nernst calorimeter operating between 2 and 100 K. A pellet of about 66 mg was used for this experiment.

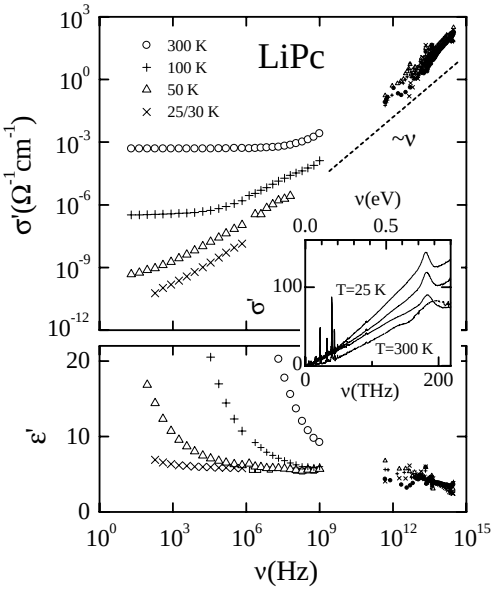

Fig. 1. Conductivity σ' and dielectric constant ϵ' in LiPc as a function of frequency at different temperatures as indicated. The inset shows the optical conductivity in the FIR spectral range at $T = 25$ K, 50 K, 100 K, and 300 K.

3 Results and discussion

3.1 Optical conductivity

The frequency dependences of the optical conductivity $\sigma'(\nu)$ and of the dielectric constant $\epsilon'(\nu)$ in LiPc and LiPcI are shown in Figures 1 and 2 for several temperatures together with the results from ac measurements at lower frequencies which were published earlier [12]. Due to the fact that we used pressed pellets, we could not separate the conductivity spectra along and perpendicular to the chain direction.

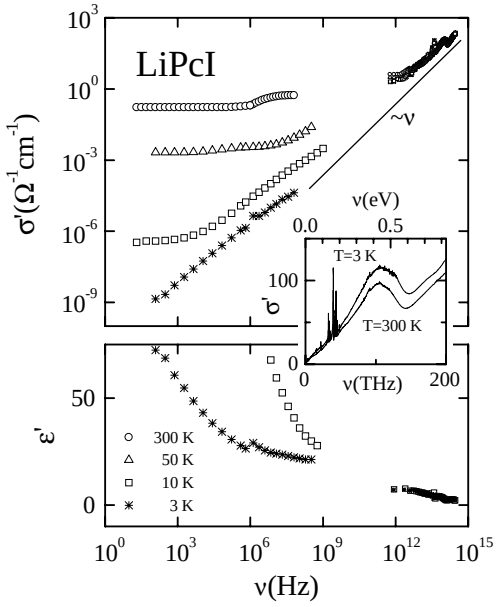

Fig. 2. Frequency dependence of the conductivity σ' and the dielectric constant ϵ' in LiPcI at different temperatures. The inset shows the optical conductivity at $T = 3$ K and 300 K in a linear scale.

Our results do not reveal the spectra expected for conventional semiconductors with the onset of absorption at the band gap. Instead, in both compounds we observe clear experimental evidence for hopping conductivity which extends from the radio frequency range well into the IR frequency regime. The conductivities in both compounds (upper frames in Figs. 1 and 2) reveal a transition from frequency independent dc transport at low frequencies to frequency dependent ac transport at high frequencies. With decreasing temperatures the transition region is shifted to lower frequencies. The ac conductivity follows a characteristic power law $\sigma(\nu) \propto \nu^s$ ($s \approx 1$), which usually is ascribed to hopping processes of localized charge carriers. This has been discussed in detail in a previous contribution [12]. Astonishingly this hopping conductivity extends well into the far-infrared (FIR) and mid-infrared (MIR) spectral range. In LiPc at higher frequencies ($\nu > 10^{13}$ Hz) there is some evidence for a transition into a regime in which the hopping processes are assisted by phonons [17]. Here, the conductivity depends quadratically ($s \approx 2$) on the measuring frequency. In the optical range of frequency we find a small and smooth increase of conductivity with decreasing temperature in contrast to the low frequency results where the conductivity depends almost linearly on temperature in agreement with predictions from phonon-activated hopping. The conductivity in the FIR range is shown separately in the insets of Figures 1 and 2. The sharp peaks below 50 THz superimposed on the smooth background are due to molecular vibrations and will not be discussed further. The phonon spectra of both compounds look similar and for LiPc good agreement with previous measurements has been found [4].

The lower frames of Figures 1 and 2 show the dielectric constants for both compounds as a function of frequency. At high temperatures and low frequencies $\epsilon'(\nu)$ is dominated by dc contributions. The true values of ϵ_∞ are reached at high frequencies and are close to 3 for both compounds. This is a rather low value taking the optical gap into consideration.

In the near-infrared spectral range both materials show a weak but significant feature in $\sigma'(\nu)$ which we attribute to excitations across an optical gap (see insets in Figs. 1 and 2). The gap values are approximately 0.75 eV in the case of LiPc and about 0.43 eV for LiPcI. In agreement with this fact we observe a larger value of the low frequency dielectric constant ϵ' in LiPcI compared to LiPc. From the distinctly different temperature dependences of these excitations across the gap we conclude that different underlying mechanisms are responsible for the gap formation. While the gap excitation in LiPcI changes only slightly with temperature, we find that in LiPc the gap excitation becomes smeared out as the temperature increases. These observations would give first experimental evidence that LiPcI is dominated by an intrinsic band gap while in LiPc the gap is due to electronic correlations.

Both compounds reveal semiconducting properties, *i.e.*, the dc resistivity increases with decreasing temperature [12]. LiPc – on the one hand – is characterized by an electron delocalized on the inner ring of the phthalocyanine molecule and can be described as a one-dimensional metal with a half-filled conduction band [8]. In contrast to metallic phthalocyanines which show a Drude-like optical conductivity along the chain direction, the conductivity in lithium phthalocyanine is suppressed *via* an on-site Coulomb repulsion and hence, LiPc becomes a one-dimensional Mott-Hubbard insulator [11]. The gap energy between the lower and the upper Hubbard band is determined to be 0.75 eV. Our value of the Hubbard gap is somewhat larger than the one (0.5 eV) reported from room-temperature optical experiments on single crystals of the tetragonal phase [11]. The gap energy does not change significantly with temperature; however, the feature becomes much sharper as the material is cooled down. This cannot solely be explained by thermal broadening since the temperature is one to two orders of magnitude smaller than the Hubbard gap.

On the other hand, LiPcI is an intrinsic band semiconductor. The linear chains of equidistant iodine atoms which are located in between the LiPc stacks have removed the extra electron and $[(\mathrm{LiPc})^+ – \mathrm{I}^-]$ is the realistic description for this iodine inclusion complex [18]. The lack of any temperature dependence in the high frequency conductivity spectrum is in accordance with the fact that for a band semiconductor we do not expect a strong temperature dependence of the optical properties for $k_B T \ll h\nu \approx E_{gap}$. Due to a large defect concentration and/or a large amount of structural disorder in both compounds, hopping conductivity dominates throughout the low frequency range up to the band gap.

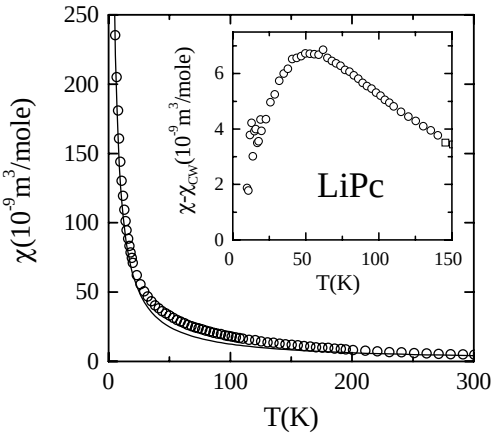

Fig. 3. Temperature dependence of the dc susceptibility in LiPc. The solid line represents a Curie fit. The inset shows the susceptibility after the Curie fit has been subtracted.

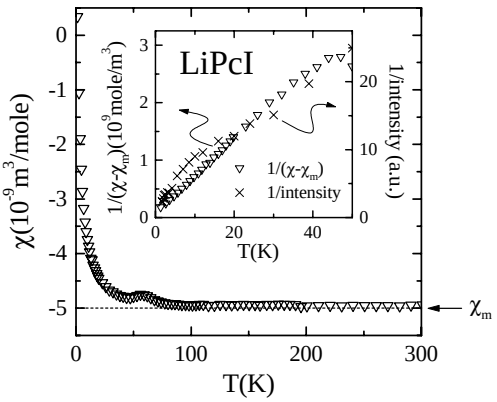

Fig. 4. Temperature dependence of the dc susceptibility in LiPcI. The dashed line indicates the calculated diamagnetic susceptibility of LiPcI as described in the text. The inset shows the inverse of the susceptibility after the diamagnetic contribution has been removed (open triangles). The crosses indicate the spin susceptibility as observed in the ESR experiments.

3.2 Magnetic susceptibility

The dc magnetic susceptibility of LiPc is shown in Figure 3. At first sight LiPc reveals a normal three-dimensional paramagnetic behavior. This is consistent with earlier observations [7,14]. However, there is a transition from a Curie-Weiss behavior $\chi = C/(T - \Theta)$ with Weiss temperature $\Theta = -30$ K at high temperatures to a Curie behavior at $T < 30$ K, indicative for the presence of paramagnetic defect states. The inset of Figure 3 shows the susceptibility data after the Curie tail has been subtracted. The susceptibility now obtained reveals a broad maximum at approximately 50 K which is an indication of low-dimensional antiferromagnetic behavior. Due to large error bars introduced by the substraction of the Curie-tail we do not want to analyze these data further. We only can state that after this correction they are consistent with the

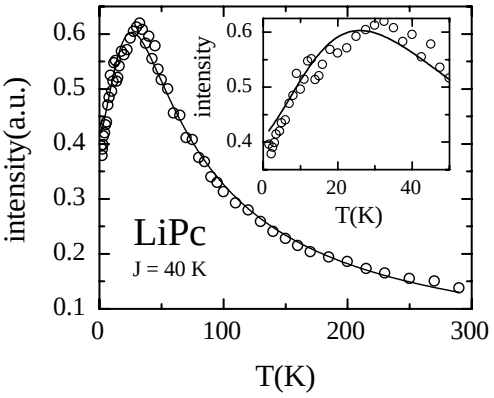

Fig. 5. Spin susceptibility of LiPc as determined *via* the ESR intensity as a function of temperature. The solid line is a fit using the Bonner-Fisher model for a $S = 1/2$ antiferromagnetic linear chain. The inset shows an enlarged section of the spin susceptibility below 50 K.

ESR results. The dc magnetic susceptibility of LiPcI shows diamagnetic behavior at high temperatures and a Curie tail due to impurities at low temperatures (Fig. 4). We determined the temperature independent molecular diamagnetic susceptibility $\chi_m \approx -5 \times 10^{-9}$ m^3/mole. Using the known value for H_2Pc ($\chi_m = -4.32 \times 10^{-9}$ m^3/mole [19]) we calculated the diamagnetic susceptibility of LiPc and LiPcI yielding $\chi_m = -4.3 \times 10^{-9}$ m^3/mole and $\chi_m = -4.96 \times 10^{-9}$ m^3/mole, respectively. The value for LiPcI is in good agreement with the experimental result.

The observed ESR signal of LiPc consists of a single small resonance line. There is no angular dependence of the resonance position H_{res} and the linewidth (half-width at half-height) ΔH. The signal is well fitted by a Lorentzian line with ΔH =700 mOe and a g-shift $\Delta g = g - 2.0023 = -0.0003$ at room temperature. No indications for a fine structure could be observed. The temperature dependence of the intensity of the ESR signal (area under absorption curve) which directly corresponds to the spin susceptibility is shown in Figure 5. With decreasing temperature, the intensity increases to a maximum at around 30 K and then falls to a finite value at low temperatures. This is a clear signature of a spin 1/2 Heisenberg antiferromagnetic linear chain. Bonner and Fisher [20] studied the magnetic and thermal properties of a $S = 1/2$ AFM linear chain. The magnetic susceptibility of such a system can be estimated at temperatures $T > 0.2J$ numerically by [21]

$$\chi(T) = \frac{Ng^2\mu_B^2}{k_B T} \frac{0.25 + 0.074975x + 0.075235x^2}{1 + 0.9931x + 0.172135x^2 + 0.757825x^3},$$

where $x = J/T$ and J is the exchange constant. For temperatures 10 K $\leq T \leq$ 300 K this equation can satisfactorily be fitted to the intensities. The exchange constant is given by $J = 40$ K. Below 10 K the intensity decreases stronger than expected for a one-dimensional spin chain.

The temperature dependences of the linewidth and of the g-shift are shown in Figure 6. In the high temperature region the linewidth ΔH slowly narrows with decreasing

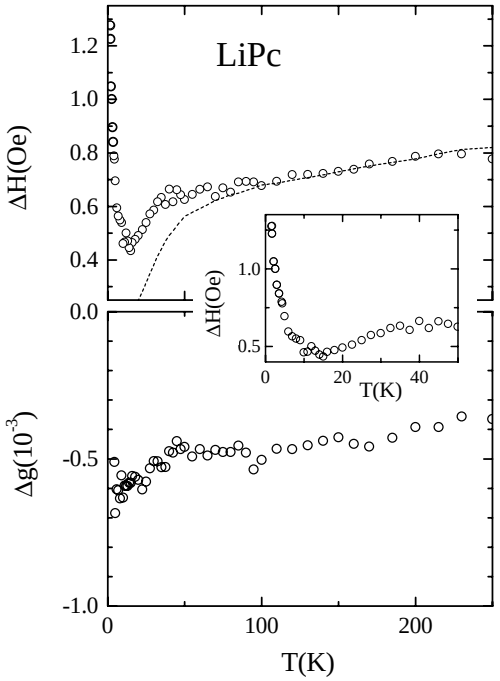

Fig. 6. Temperature dependence of the linewidth ΔH (upper frame) and g-shift (lower frame) of the ESR resonance absorption as observed in LiPc. The dashed line represents χT normalized at 200 K and indicates the contribution of the long-wavelength modes to ΔH at higher temperatures. The inset emphasizes the low temperature region of $\Delta H(T)$.

temperature. For $T \leq 40$ K the slope of ΔH *versus* T first increases and than the linewidth reaches a minimum at $T \approx 15$ K with $\Delta H_{min} = 430$ mOe before it broadens strongly. The low temperature behavior is shown on an enlarged scale in the inset of Figure 6. The negative g-shift shows a weak temperature dependence. It steadily decreases down to the lowest temperatures. The small value of the linewidth in the whole temperature range indicates a rather low dimensionality. A similar behavior in the temperature dependence of ΔH was observed earlier in one-dimensional $S = 1/2$ Heisenberg antiferromagnets like $CuCl_2{\cdot}2NC_5H_5$ as well as in classical spin chains like $CsMnCl_3{\cdot}2H_2O$ [22,23]. The high temperature behavior indicates that fluctuations with wave vector $q \to 0$ which are slowly decaying with temperature dominate the relaxation process at higher temperatures. Following the one-dimensional spin-diffusion theory, the temperature dependence of the contribution of this long-wavelength $q \to 0$ modes is given by $\Delta H_{q\to 0} \propto \chi T$ [23]. In the upper part of Figure 6, χT is scaled to ΔH at $T = 200$ K. There is a good agreement with $\Delta H(T)$ above $T \approx 100$ K. The low temperature behavior of the linewidth can be explained by the onset of short-range antiferromagnetic spin correlations for temperatures $T < J$. There is an additional contribution of staggered susceptibility modes which causes an rapid increase of the linewidth with decreasing temperature.

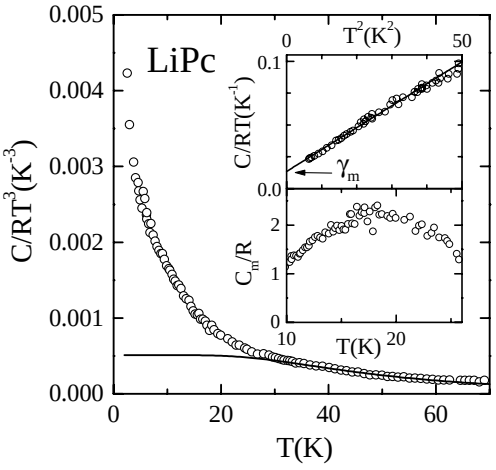

Fig. 7. Heat capacity in units of the gas constant R for LiPc plotted as C/T^3 *vs.* T. The solid line was calculated on a Debye model. Upper inset: The low temperature part ($T < 7$ K) of the heat capacity was plotted as C/T *vs.* T^2. The straight line has been calculated with a linear magnetic contribution as predicted for temperatures $T \ll J \approx 40$ K. Lower inset: Temperature dependence of the heat capacity C_m with the lattice contribution subtracted. The magnetic contribution to the heat capacity shows a maximum at $T_{max} \approx 18$ K.

LiPcI reveals a weak ESR signal. It is smaller by a factor of 10 to 20 compared to the signal in LiPc but shows the same line shape and a similar temperature dependence. The ESR intensity in LiPcI scales well with the Curie-Weiss tail from the dc experiments (see inset in Fig. 4). Hence, the observed ESR signal results from paramagnetic defect states (mostly LiPc residues). Thus it is obvious that pure LiPcI is ESR silent with no free radical electron. Our result confirms that LiPcI is a fully oxidized metallophthalocyanine with one-dimensional arrays of iodine, present in the voids, as predicted in [18], in contrast to partially oxidized highly conducting metallophthalocyanines like NiPcI with triiodide (I_3^-) chains.

3.3 Specific heat

The heat-capacity measurements on LiPc for 3 K$< T <$ 70 K are shown in Figure 7. Spin systems like LiPc have two contributions to the total heat capacity C, the lattice contribution C_l and the magnetic contribution C_m. The lattice contribution was determined using the Debye integral in which the specific heat at any temperature can be calculated in terms of the Debye temperature Θ_D. For calculating C_l we have used the heat-capacity data in the temperature range between 35 and 60 K. The solid line in Figure 7 represents a Debye fit with $\Theta_D = 218$ K. The derivations from the fit in the C/T^3 *versus* T plot below 25 K are caused by the magnetic contribution C_m to the heat capacity of a $S = 1/2$ AFM linear spin chain. Following Bonner and Fisher [20], at low temperatures C_m increases linearly with temperature, then rises to a maximum at $T/J = 0.48$, and finally decreases with increasing temperatures. The magnetic contribution

to the heat capacity at low temperatures ($T/J < 0.1$) was calculated using the Bethe ansatz [24] and is given by $C_m = \gamma_m T = 2RT/3J$ where R is the molar gas constant.

Hence at low temperatures the heat capacity in LiPc can be described by $C = \gamma_m T + aT^3$. The upper inset of Figure 7 shows C/T *versus* T^2. In this representation the finite value at $T = 0$ K gives the coefficient of the linear term γ_m. We find $\gamma_m/R = 0.014$ K^{-1} and $J \approx 47$ K. Between 10 K $\leq T \leq$ 25 K C_m shows the predicted maximum at $T_{max} \approx 18$ K (Fig. 7, lower inset) which corresponds to a next-nearest neighbor exchange $J \approx 38$ K. Both results are in agreement with the result derived from the ESR measurements. However, it should be mentioned that the maximum is by a factor of 6 too high compared to the theoretical predictions. A possible reason for this deviation could be the fact that the modeling of the lattice contribution to the heat capacity by a temperature independent Θ_D is an oversimplified assumption.

4 Conclusions

We have studied the magnetic and electrodynamic properties of powder samples of the one-dimensional organic semiconductors LiPc and LiPcI. The frequency dependence of the conductivity exhibits a power-law behavior ν^s over a wide range of frequency indicating hopping conduction as the main transport mechanism. In both compounds we observe excitations across an energy gap. While LiPcI is a band semiconductor, LiPc is found to be a Mott-Hubbard insulator due to strong electronic on-site correlations. The temperature dependence of the intensity of the ESR signal, which is proportional to the spin susceptibility, as well as the magnetic contribution to the heat capacity are well described by a spin 1/2 one-dimensional antiferromagnetic Heisenberg chain model. The exchange energy is given by $J \approx 40$ K. LiPcI is ESR silent indicating that all the unpaired electrons have been removed from the macrocycle.

The work at Augsburg was supported by the BMBF under the contract number EKM 13N6917.

References

1. T.J. Marks, Science **227**, 881 (1985).
2. *Phthalocyanines: Properties and Applications*, edited by C.C. Leznoff, A.B.P. Lever (VCH, New York, 1989-1996), Vols. 1–4.
3. M. Hanack, M. Lang, Adv. Mater. **6**, 819 (1994).
4. H. Homborg, W. Katz, Z. Naturforsch. **33b**, 1067 (1978).
5. P. Turek, J.-J. André, A. Giraudeau, J. Simon, Chem. Phys. Lett. **134**, 471 (1987).
6. H. Sugimoto, M. Mori, H. Masuda, T. Taga, J. Chem. Soc. Commun. 962 (1986).
7. P. Turek, M. Moussavi, J.-J. André, Europhys. Lett. **8**, 275 (1989).
8. E. Orti, J.L. Brédas, C. Clarisse, J. Chem. Phys. **92**, 1228 (1990).
9. P. Turek, P. Petit, J.-J. André, J. Simon, R. Even, B. Boudjema, G. Guillaud, M. Maitrot, J. Am. Chem. Soc. **109**, 5119 (1987).
10. P. Turek, M. Moussavi, P. Petit, J.-J. André, Synth. Met. **29**, F65 (1989).
11. K. Yakushi, T. Ida, A. Ugawa, H. Yamakado, H. Ishii, H. Kuroda, J. Phys. Chem. **95**, 7636 (1991).
12. M. Dumm, P. Lunkenheimer, A. Loidl, B. Assmann, H. Homborg, P. Fulde, J. Chem. Phys. **104**, 5048 (1996).
13. M. Dumm, R. Spitzfaden, P. Lunkenheimer, M. Dressel, A. Loidl, B. Assmann, H. Homborg, P. Fulde, Synth. Met. **84**, 925 (1997).
14. P. Turek, J.-J. André, J. Simon, Solid State Commun. **63**, 741 (1987).
15. F. Bensebaa, J.-J. André, J. Phys. Chem. **96**, 5739 (1992).
16. H. Homborg, C.L. Teske, Z. Anorg. Allg. Chemie **527**, 45 (1985).
17. N.F. Mott, E.A. Davis, *Electronic Processes in Non-Crystalline Materials*, 2nd edn. (Clarendon Press, Oxford, 1979).
18. B. Latte, A. Kienast, C. Bruhn, A. Loidl, H. Homborg, J. Porphy. Phthalocyan. **1**, 267 (1997).
19. C.G. Barraclough, R.L. Martin, S. Mitra, J. Chem. Phys. **55**, 1426 (1971).
20. J.C. Bonner, M.E. Fisher, Phys. Rev. **135**, A640 (1964).
21. W.E. Estes, D.P. Gavel, W.E. Hatfield, D. Hodgson, Inorg. Chem. **17**, 1415 (1978).
22. Y. Tazuke, K. Nagata, J. Phys. Soc. Jpn **38**, 1003 (1975).
23. Y. Ajiro, S. Matsukawa, T. Yamada, T. Haseda, J. Phys. Soc. Jpn **39**, 259 (1975).
24. H.M. Babujian, Nucl. Phys. B **215**, 317 (1983).